Investigation of the Breakaway Oxidation Phenomenon for Zircaloy-4 Oxidized at 1000℃

Dong Jun Park*, Jeong Yong Park, Byoung Kwon Choi, Yong Hwan Jeong,
Nuclear Convergence Technology Division, Korea Atomic Energy Research Institute, 1045 Daedeok-daero, Yuseong-gu, Daejeon 305-353, Korea
**Corresponding author: pdj@kaeri.re.kr*

1. Introduction

It is very important for Zr cladding to maintain its fuel integrity in a postulated design-based accident, as well as during a normal operation. If a loss-of-coolant accident (LOCA) which is one of the most important design-basis accidents occurs, then Zr alloy cladding would be exposed to steam at high temperatures until it is quenched by emergency core cooling water [1]. Subsequently, significant cladding oxidation takes place on the surface of the cladding tube during the LOCA, and prolonged exposure to steam can cause breakaway oxidation which is described by linear oxidation kinetics with a sudden increase in the oxidation rate which follows initial parabolic regimes [2]. This phenomenon severely promotes embrittlement of the cladding, therefore it is very important to explain precisely why this breakaway oxidation takes place during the LOCA for safety analysis. In this study, we attempted to synthesize the microstructure of the oxide layer formed on Zircaloy-4 tube at a temperature of 1000℃ by using a high resolution TEM (HRTEM). As a result, we observed flat grain boundaries (GBs) and micropores between the enlarged grains in post-breakaway oxide layer. We propose a mechanism to explain how these microstructural changes play a crucial role in transition to the breakaway and contribute to the enhanced oxidation rate.

2. Methods and Results

2.1 Experimental Procedure

A Zircaloy-4 tube which has a 200 mm length was used in this study. Direct heating by an ohmic resistance enabled the specimen to heat up to temperatures of 1000℃. Specimen temperature was measured by a pyrometer. The specimen was oxidized in a flowing steam with different exposure times in the range of 300 s to 4000 s. Finally, the specimen was cooled at an intermediate temperature of 700℃ for 200 s after oxidation and then quenched. The metallographic study and cross sectional morphology of the oxide layer was investigated by optical microscopy (OM) with a polarized filter, and the HRTEM (JEM 3010) operated at 300 kV. TEM samples sectioned from the oxidized tube were polished mechanically and then argon ion thinned for electron transparency.

2.2 Results

Fig. 1 shows the morphology of the ZrO_2 layers formed on the Zr tube with different oxidation times of 300 s (sample A), 3000 s (sample B), and 4000 s (sample C). Sample A showed a uniform oxide layer with a mean thickness of 41.7 ㎛. Thickness of the oxide layer increased slightly up to an oxidation time of 3000 s, but sample C showed a sudden increase in the thickness of the oxide layer due to breakaway oxidation. The lateral crack parallel to the interface between oxide and metal (see arrow in Fig. 1(c)) was formed during the transition to breakaway oxidation. Based on results of the previous report [5], it seems likely that the oxide layer below the arrow is the black hypostoichiometric oxide (anion-deficient) and the upper one is the white (or grey) stoichiometric oxide.

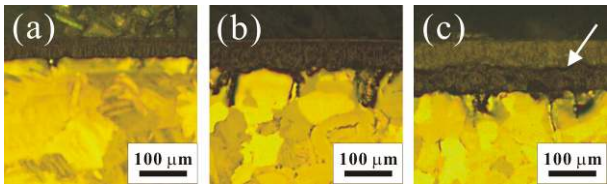

Fig. 1. Optical metallographs of outer surface oxide layers oxidized at 1000℃ with different oxidation times: (a) 300 s, (b) 3000 s, and (c) 4000 s.

Cross-sectional bright field TEM images of the oxide layer from samples A and C are shown in Figs. 2(a) and (b). While sample A showed high density columns vertically aligned with round tips, enlarged grains having fine pores in GBs (see arrows and inset of Fig. 2(b)) were observed in sample C. Selected area diffraction patterns (SADPs) obtained from both samples indicate that oxide layers of sample A and C are composed of two mixed crystallographic forms of the tetragonal and monoclinic phase. However, it is not absolutely clear due to very similar interplanar spacing distances of several planes of the two crystallographic phases, such as the (200) plane of monoclinic ZrO_2 and the (110) plane of tetragonal ZrO_2. The SADP was converted from an initial ring pattern to a spotty one. These results reveal that crystallinity and the size of grains in the oxide layer changed during breakaway oxidation, i.e., small grains having a random distribution in crystalline orientation changed to large grains with high crystallinity and the same crystalline orientation due to a longer oxidation time at a high temperature.

Based on TEM observation, a schematic diagram is depicted in Fig. 3. In contrast to the oxide layer formed at a pre-breakaway transition with unclear and uneven GBs

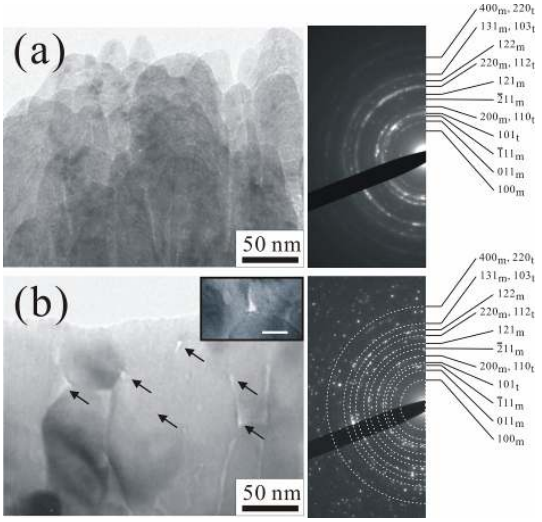

Fig. 2. Cross-sectional bright-field TEM micrographs obtained from the oxide layers of (a) sample A and (b) C. The inset of (b) shows the enlarged TEM image of a grain boundary containing a micro-pore, and the scale bar denotes 20 nm. Corresponding SADPs of the oxide layer are shown on the right of each BF TEM image.

[Fig. 3(a)], breakaway oxidation transition led to the formation of enlarged grains having flat and clear GBs, resulting in enhanced oxygen diffusion into the oxide layer [Fig. 3(b)]. This can be explained by the fact that GBs could be a short circuit associated with easier diffusion paths, as indicated by heavy arrows in Fig. 3(b). That is, the GB with mismatch between adjacent crystal grains in the material's microstructure is a more open structure, allowing enhanced diffusion [3,4]. The relative diffusivities are $D_{\text{volume}} < D_{\text{grain boundary}} < D_{\text{surface}}$. Furthermore, micropores located at grain triple points and GBs are also open structures. For the crack formation during breakaway oxidation, micropores can increase the magnitude of the local stresses or cause a crack which appear to spread from the internal micropores to the GBs [5]. Thus, these micropores are considered to be the origin of the mechanical cracks in the oxide layer during breakaway oxidation. In addition, flat GBs in sample C are more favorable to crack propagation occurring during transition to breakaway oxidation than uneven GBs in sample A.

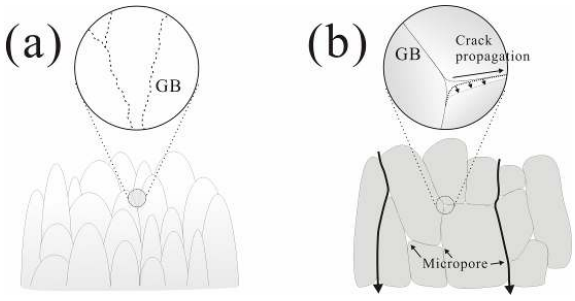

Fig. 3. Schematic diagrams of (a) the oxide layer formed at pre-breakaway kinetics, and (b) the oxide layer formed during the transition to breakaway oxidation.

3. Conclusions

We demonstrated breakaway oxidation behavior and resulting microstructural changes of the oxide layer formed on the Zircaloy-4 tube at 1000℃ with a different oxidation time. Oxide layers with small grains showing unclear and uneven GBs were grown at a shorter oxidation time, whereas larger grains with flat GBs and micropores were observed in the oxide layer grown during transition to breakaway oxidation. Based on the microstructural changes affecting breakaway such as the shape of GBs and the formation of micropores, a mechanism was proposed to explain the process of breakaway oxidation transition.

REFERENCES

[1] F. Nagase and T. Fuketa, Fracture Behavior of Irradiated Zircaloy-4 Cladding under Simulated LOCA Conditions, Journal of Nuclear Science and Technology, Vol. 43, p. 1114 2006.
[2] G. R. Wallwork, C. J. Rosa, and W. W. Smeltzer, Breakaway phenomena in the oxidation of zirconium at 850 and 950℃, Corrosion Science, Vol. 5, p. 113 1965.
[3] J.F. Shackelford, Introduction to Materials Science for Engineers, 3nd ed., Macmillan Publishing Company, New York, pp.127-129, 1985.
[4] A.E. Paladino and W.D. Kingery, Aluminum Ion Diffusion in Aluminum Oxide, The Journal Chemical Physics, Vol 37, p. 957 1962.
[5] L. Ewart, S. Suresh, Crack Propagation in Ceramics under Cyclic Loads, Journal of Materials Science, Vol. 22, p. 1173 1987.